ACCOUNTS
of chemical research

# Computational Analysis of the Mechanism of Chemical Reactions in Terms of Reaction Phases: Hidden Intermediates and Hidden Transition States

ELFI KRAKA* AND DIETER CREMER

*Department of Chemistry, Southern Methodist University, 3215 Daniel Avenue, Dallas, Texas 75275-0314*

RECEIVED ON JANUARY 9, 2009

## CONSPECTUS

Computational approaches to understanding chemical reaction mechanisms generally begin by establishing the relative energies of the starting materials, transition state, and products, that is, the stationary points on the potential energy surface of the reaction complex. Examining the intervening species via the intrinsic reaction coordinate (IRC) offers further insight into the fate of the reactants by delineating, step-by-step, the energetics involved along the reaction path between the stationary states.

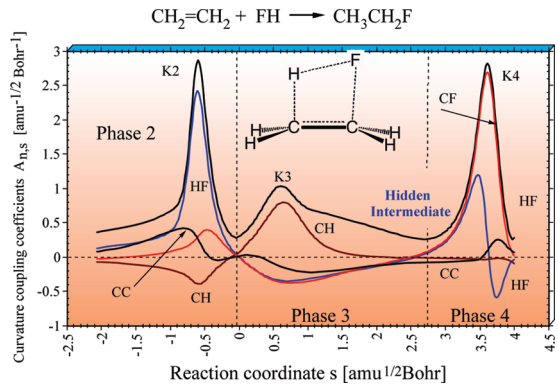


For a detailed analysis of the mechanism and dynamics of a chemical reaction, the reaction path Hamiltonian (RPH) and the united reaction valley approach (URVA) are an efficient combination. The chemical conversion of the reaction complex is reflected by the changes in the reaction path direction $\mathbf{t}(s)$ and reaction path curvature $\mathbf{k}(s)$, both expressed as a function of the path length $s$. This information can be used to partition the reaction path, and by this the reaction mechanism, of a chemical reaction into reaction phases describing chemically relevant changes of the reaction complex: (i) a contact phase characterized by van der Waals interactions, (ii) a preparation phase, in which the reactants prepare for the chemical processes, (iii) one or more transition state phases, in which the chemical processes of bond cleavage and bond formation take place, (iv) a product adjustment phase, and (v) a separation phase. In this Account, we examine mechanistic analysis with URVA in detail, focusing on recent theoretical insights (with a variety of reaction types) from our laboratories.

Through the utilization of the concept of localized adiabatic vibrational modes that are associated with the internal coordinates, $q_n(s)$, of the reaction complex, the chemical character of each reaction phase can be identified via the adiabatic curvature coupling coefficients, $A_{n,s}(s)$. These quantities reveal whether a local adiabatic vibrational mode supports ($A_{n,s} > 0$) or resists ($A_{n,s} < 0$) the curving of the path, and thus the structural changes of the reaction complex.

URVA can show the mechanism of a reaction expressed in terms of reaction phases, revealing the sequence of chemical processes in the reaction complex and making it possible to determine those electronic factors that control the mechanism and energetics of the reaction. The magnitude of adiabatic curvature coupling coefficients is related to strength and polarizability of the bonds being broken. Transient points along the reaction path are associated with hidden intermediates and hidden transition states, which can be converted into real intermediates and transition states when the reaction conditions or the substitution pattern of the reaction complex are appropriately changed. Accordingly, URVA represents a theoretical tool with tremendous experimental potential, offering the chemist the ability to assert greater control over reactions.

## 1. Introduction

The major goal of chemistry is to control chemical reactions. This implies detailed knowledge of the reaction mechanism and how the latter can be manipulated to reduce the reaction barrier, improve stereoselectivity, increase product yield, or suppress undesirable side reactions. Controlled changes of this nature are often needed when optimizing the production of valuable new materials from abundantly available

Published on the Web 03/16/2010 www.pubs.acs.org/acr
10.1021/ar900013p 

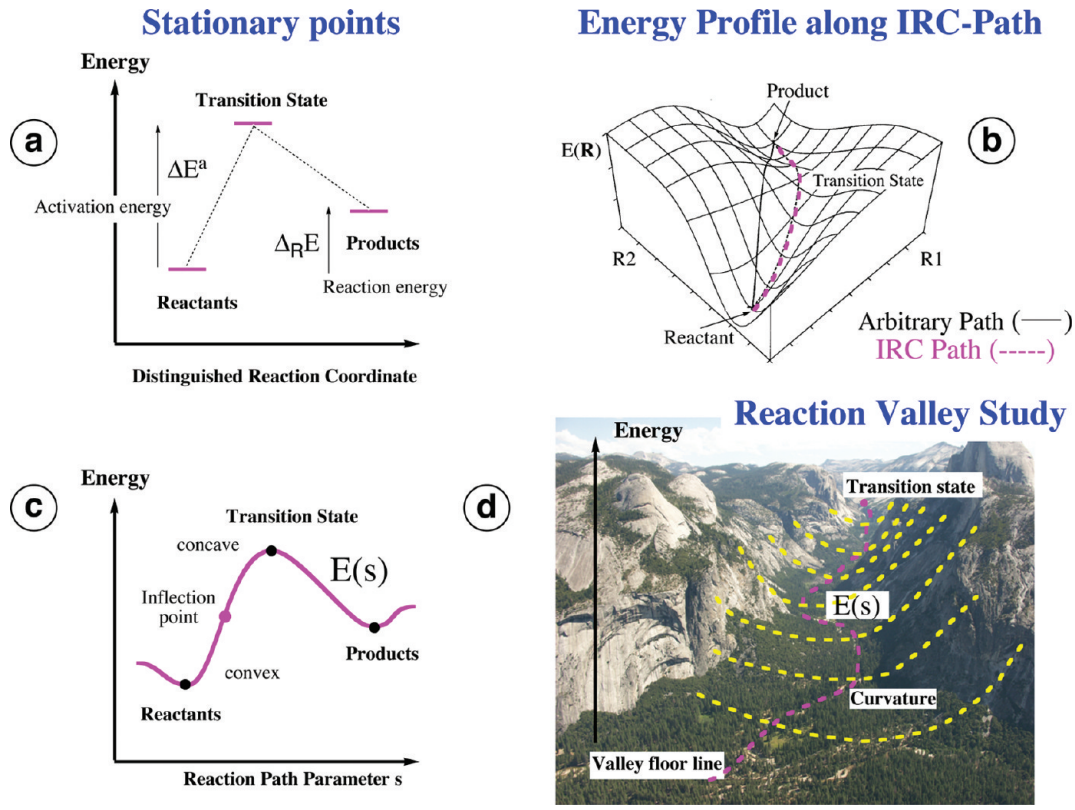


**FIGURE 1.** Three ways of investigating the mechanism of a chemical reaction computationally: (a) investigation of stationary points; (b) additional investigation of the IRC path connecting the stationary points; (c) energy profile along the IRC path of panel b; convex and concave parts of *E*(*s*) are indicated; (d) investigation of reaction path and reaction valley embedding the path.

resources at low energy cost without jeopardizing our environment.

For more than a century, chemists have measured activation enthalpies and reaction rate constants to learn about the properties of chemical reactions with the goal of controlling them.[1,2] Quantum chemical methods have provided the possibility of calculating the properties of transition states and reaction intermediates not amendable to experiment[3] or determining reaction rates by combining quantum chemistry with suitable reaction dynamics methods.[4]

Today one can distinguish among three different computational approaches for describing, analyzing, and understanding the mechanism of a chemical reaction (see Figure 1): (a) The stationary points located on the potential energy surface (PES) of the reaction complex and corresponding to reactant minimum, first-order saddle point (transition state), and product minimum of a chemical reaction are calculated. This leads to the energetics of the reaction, gives some insight into the mechanism, and is done in the majority of all quantum chemical investigations. (b) The intrinsic reaction coordinate (IRC) path of Fukui,[5] which is the steepest descent path in mass-weighted coordinates connecting the transition state with reactants and products, is computed. For a complicated mechanism (e.g., see the investigation of the ozone−acetylene reaction[6]), it is no longer possible to assess the topology of a PES from stationary points alone. IRC calculations have to clarify which stationary points are connected by one and the same reaction path. (c) For studying mechanism and dynamics of a chemical reaction in detail the (classical) reaction path Hamiltonian (RPH) of Miller, Handy, and Adams[7] can be used as an underlying mathematical concept. The RPH is based on a partitioning of the $(3N - 6)$ dimensional PES ($N$ = number of atoms of the reaction complex) close to the reaction path into the one-dimensional minimum energy path and the $(3N - 7)$-dimensional reaction valley embedding the reaction path. This is the basis of the unified reaction valley approach (URVA),[8−12] which provides a detailed account of the changes of electronic and geometrical structure of the reaction complex by exploring reaction path and valley from entrance to exit channel.[11,13−18] In the following, we will consider exclusively the third approach of analyzing the mechanism of a chemical reaction.

## 2. Basics of Reaction Mechanism

Detailed insight into the mechanism of a chemical reaction requires the knowledge of how the properties of the reaction complex change along a representative reaction path. In the

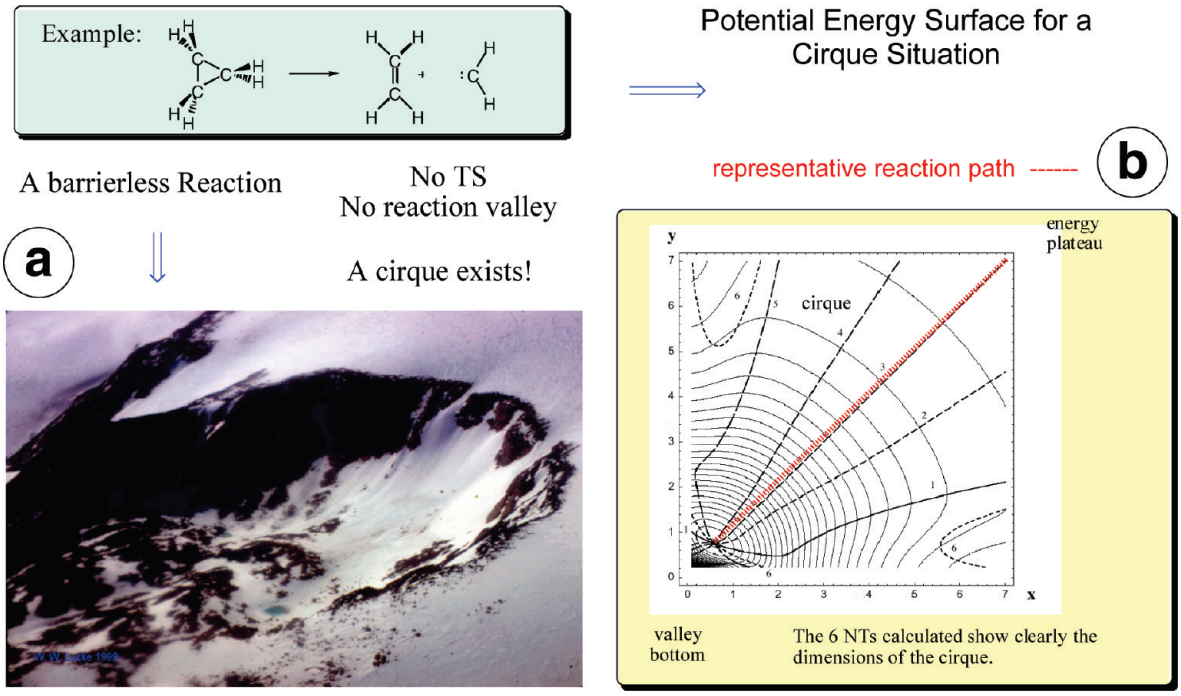


**FIGURE 2.** Schematic representation of a PES resembling that of the methylene−ethene cycloaddition reaction complex. Reaction energy, $\Delta E = -112.1$ kcal/mol; $\Delta H(298) = -105.6$ and $\Delta H(298,\text{exp}) = -101.6$ kcal/mol.[18] (a) Geographical cirque; (b) model surface with minimum at the lower left corner (corresponding to cyclopropane) and energy plateau in the upper right corner (corresponding to methylene + ethene). Newton trajectories (NT, dashed lines) trace out possible paths from the energy minimum to the energy plateau.[18]

literature, different reaction paths have been suggested[5,19,20] where one has to consider that the reaction path is, similar to the chemical bond, just a model quantity based on the concept of the PES. The IRC path[5] expressed as a function of its arclength, $s$, provides a suitable choice of a representative path. Usually the IRC tends to follow the floor line of the reaction valley (especially in regions where the function $E(s)$ is convex[19]) leading from reactants to transition state and products.

There are reactions that possess such a small energy barrier that after considering vibrational and temperature corrections, the activation enthalpy, $\Delta H^a$, vanishes. Although such a transition state is not chemically relevant, it can be used for the determination of an IRC path and the mechanistic analysis. The addition of vinylidene to acetylene yielding methylenecyclopropene represents a typical example for such a case.[12]

There are reactions (e.g., dissociation or recombination reactions) that do not possess a transition state at all, and therefore an IRC path no longer exists. Nevertheless it is possible to determine a representative path on a multidimensional PES.[12,18] Two cases can be distinguished: (a) the reaction valley disembogues into an energy plateau; (b) there is no reaction valley. The PES close to the reactant minimum resembles a cirque: From the reactant minimum, many paths ascend a bowl-shaped slope up to an energy plateau (Figure 2). The latter situation is found for the decomposition of cyclopropane to methylene and ethene; that is, the methylene−ethene cycloaddition can follow a multitude of energy-equivalent paths downhill to the cyclopropane minimum (Figure 2).[18] For cases a and b, it is possible to determine chemically meaningful paths by exploring the reaction valley close to the energy plateau or the range of the cirque with the help of Newton trajectories (Figure 2).[12,18] Once the shape of reaction valley or cirque is known, a central point at the edge of the energy plateau can serve as the starting point for a downhill path. Experience shows that such a path or related (parallel) paths lead to a representative description of the reaction mechanism.[12,18]

The dissection of the mechanism into reaction steps is energy-based as are nearly all analysis methods applied today for mechanistic studies. For example, one can determine the first derivative of the energy function $E(s)$, which leads to the reaction force, $F(s) = -dE(s)/ds$.[21,22] In this way, an $E$-based partitioning of the reaction path, given by the extrema and the zero points of the force, is possible. However, such an $E$-based partitioning of a chemical reaction misses mechanistic detail: The energy is a cumulative parameter that collects all energy changes associated with the reacting molecules in one quan-

tity thus disguising mechanistic details. It is a reliable bookkeeping quantity; however it is less useful for a detailed understanding of the reaction mechanism.

For the purpose of gaining more insight into the reaction mechanism, it is useful to focus on the *chemical processes* of bond forming and bond breaking. Clearly, more than one or two chemical processes can take place in a chemical reaction. These take place within confined ranges (described by specific *s*-values) of the reaction path, which are called bond-breaking phase, bond-forming phase, or in general *reaction phases*.[11,18]

There are other than the chemical processes that are relevant for a detailed account of the mechanism. For example, in the van der Waals phase far out in the entry (exit) channel the reactants (products) adjust their mutual positions to minimize exchange repulsion and to maximize stabilizing dispersion and electrostatic interactions. In the reactant preparation phase, the reactants prepare by undergoing conformational changes for the actual chemical processes whereas in the product adjustment phase, the products relax to a more stable form. Each reaction phase is associated with a typical change of the reaction complex. One can detail the mechanism by describing the electronic, geometrical, and dynamical changes of the reaction complex in chemically meaningful reaction phases.

The geometrical changes of the reaction complex (described by internal coordinates $q_n(s)$) determine the reaction phases because they are a direct result of the corresponding electronic changes of the reaction complex. These changes are often too difficult to analyze because the structural changes of the reaction complex can involve many *q*-coordinates and in general it is not clear which of them are most important for a detailed description of the reaction mechanism (Figure 3a). In this situation, one can take advantage of the fact that reaction path and reaction complex are closely related since the former is determined by the geometrical changes of the latter. Rather than keeping account of all geometrical changes, $\Delta q_n(s)$, of the reaction complex and identifying those that are relevant for the mechanism, the changes of the reaction complex can be described by just two essential reaction path properties: (i) the reaction path direction given by the tangent vector $\mathbf{t}(s)$[8,11,23] and (ii) the reaction path curvature given by the curvature vector $\mathbf{k}(s)$ (Figure 3b).[7,8,24] Focusing here just on the path curvature expressed as the scalar curvature, $k(s)$ (Figure 3c), it is possible to analyze $k(s)$ in terms of contributions associated with the internal coordinates, $q_n(s)$, of the reaction complex[8,11] rather than analyzing the geometrical changes of the reaction complex directly.

For this purpose, one investigates the dynamical behavior of the reaction complex, which involves the $3N - 7$ vibrational motions orthogonal to the reaction path and the translational motion along the path. Starting at the reactant minimum, a vibrational mode initiates the reaction, that is, a large amplitude vibration converts into a translational motion along the reaction path. The normal coordinates *Q* of the remaining $3N - 7$ vibrational motions of the reaction complex span the $(3N - 7)$-dimensional reaction valley. In case of reaction path curving, translational and vibrational motions can couple (Figure 3b) as described by the normal mode curvature coupling coefficients $B_{\mu,s}(s)$ (see Figure 3d) and an energy transfer between these motions can take place.[7,8,23,24] This can be used for mode-selective rate enhancement: A laser is tuned to the frequency of mode $\mu$, energy is pumped into this mode and then channeled via curvature coupling into the translational motion along the reaction path thus enhancing the reaction rate in a selective way. Knowledge of the normal mode curvature coupling coefficients is however not sufficient to prepare a mode selective rate enhancement experiment. If the mode in question couples with other vibrational modes, the excess energy can be dissipated within the reaction complex before energy transfer to the reaction mode becomes possible. Hence, one has also to know the mode−mode or Corolis coupling coefficients, $B_{\mu,\nu}(s)$[7,8,23,24] (Figure 3d) to predict the possibility of mode-selective rate enhancement.

For the mechanistic analysis, couplings $B_{\mu,s}(s)$ are of limited use because they refer to delocalized vibrational normal modes. Within URVA, they are transformed into adiabatic curvature coupling coefficients, $A_{n,s}(s)$, based on the local adiabatic internal coordinate modes[25−31] that are associated with the internal coordinates $q_n(s)$ used to describe the reaction complex (Figure 3e). Large positive or negative $A_{n,s}(s)$ indicate a chemical change of the reaction complex described by the internal coordinate $q_n(s)$. Since the sum of the squares of the curvature coupling coefficients leads to the scalar curvature (Figure 3d), curvature enhancements and peaks, *K* (Figure 3c), indicate the changes of the reaction complex and thereby the phases of the chemical reaction. Investigations reveal that in most cases just a small number of curvature coupling coefficients and internal coordinates drive the changes of the reaction complex during the reaction (Figure 3f). Hence, the

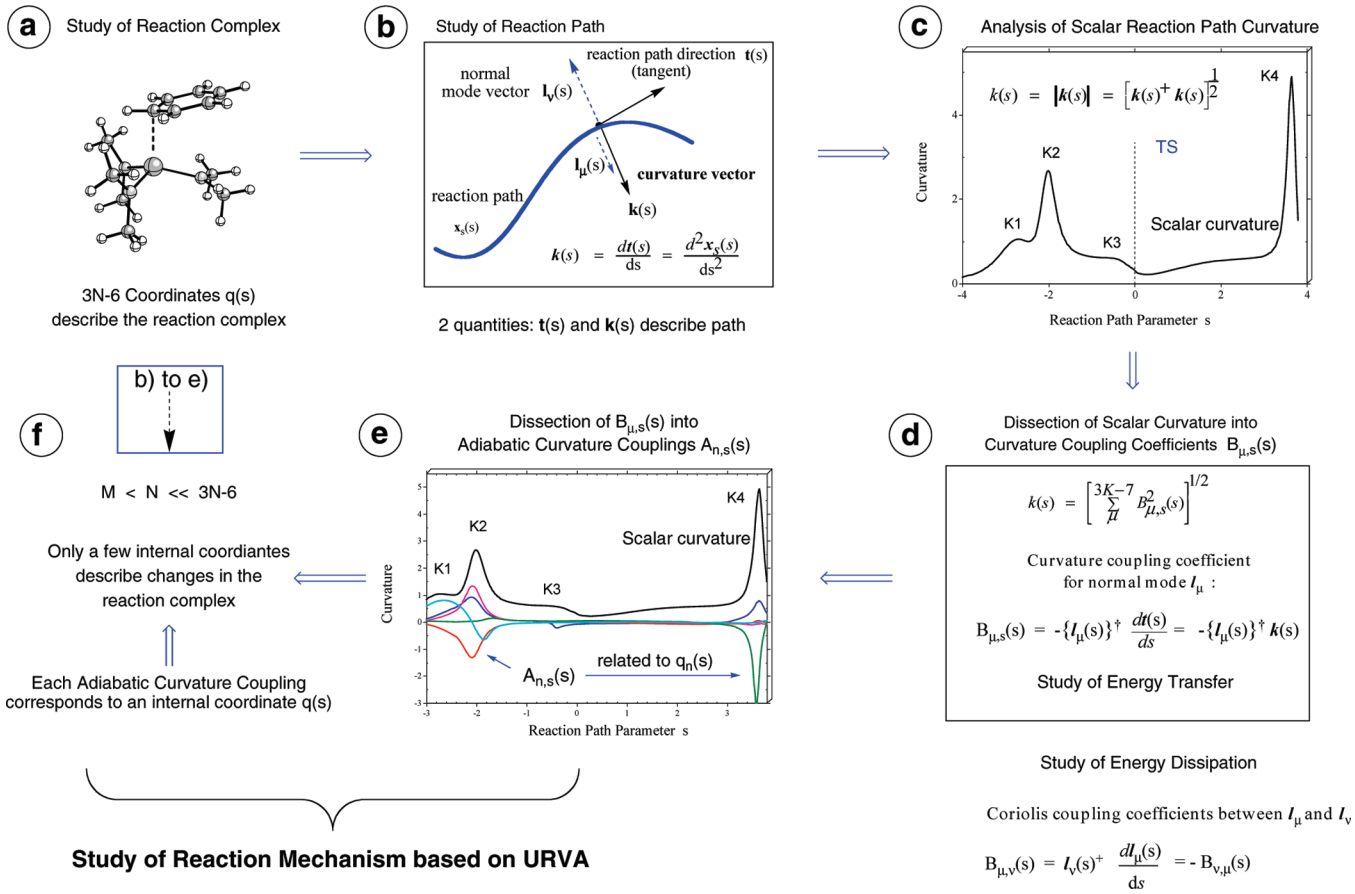


**FIGURE 3.** Strategy of a URVA analysis: (a) study of the reaction complex requires the analysis of $3N - 6$ internal coordinates, $q_n(s)$; (b) the same information is contained in the direction, $\mathbf{t}(s)$, and the curvature, $\mathbf{k}(s)$, of the reaction path; normal modes, $\mathbf{l}_\mu(s)$ or $\mathbf{l}_\nu(s)$, can couple with curvature, $\mathbf{k}(s)$, if properly aligned; (c) to obtain this information, the scalar curvature, $k(s)$, is calculated and (d) dissected into curvature coupling coefficients, $B_{\mu,s}(s)$; these are needed for studying energy transfer (for energy dissipation studies, Coriolis coefficients, $B_{\mu,\nu}(s)$, are calculated); (e) normal mode decomposition into adiabatic vibrational modes leads to adiabatic curvature couplings, $A_{n,s}(s)$, which identify all important changes of the internal coordinates, $q_n(s)$, of the reaction complex; (f) just a few ($M < N$) rather than $3N - 6$ internal coordinates have to be analyzed to describe structural changes of the reaction complex.

sequence a−f given in Figure 3 describes the mechanistic analysis principle utilized in URVA for the study of chemical reactions.

## 3. Mechanistic Analysis with the Unified Reaction Valley Approach

Use of URVA in mechanistic studies has led to an advanced understanding of chemical reactions.[8−18] URVA determines the energy profile, $E(s)$, and the reaction force, $F(s)$, as well as higher derivatives of $E(s)$, geometrical parameters, $q_n(s)$, and their derivatives, the internal forces and normal vibrational modes of the reaction complex, reaction path direction, $\mathbf{t}(s)$, and curvature, $\mathbf{k}(s)$, and normal and adiabatic mode curvature coupling and Coriolis coupling coefficients at each point $s$ along the reaction path.

The reaction path curvature of a reaction AB + C ⇔ A + BC is related to the adiabatic stretching force constant $f_a$(AB) of the bond being broken and $f_a$(BC) of the bond being formed where the changes in the $f_a(s)$ values as reflected by $f_a'(s) = df_a(s)/ds$ matter rather than their magnitudes. This is a reflection of the fact that besides the strength of bond AB also the polarizability of bond AB, the polarizing power of the reactant C, and the strength of the bond BC determine the reaction barrier. Any chemical reaction involving two or more chemical processes follows in $3N - 6$-dimensional space a reaction path with at least one curvature peak because chemical change requires a curving of the reaction path. A straight reaction path leaves the network of bonds of the reaction complex unchanged.[32]

Since the path curvature reflects the structural changes of the reaction complex, it can be analyzed to identify the chemical processes taking place and the range of the corresponding reaction phases.[11,18] The character of the reaction phase is determined by identifying the dominating adiabatic curvature coupling coefficients, $A_{n,s}(s)$ (see cycle in Figure 3). The lat-

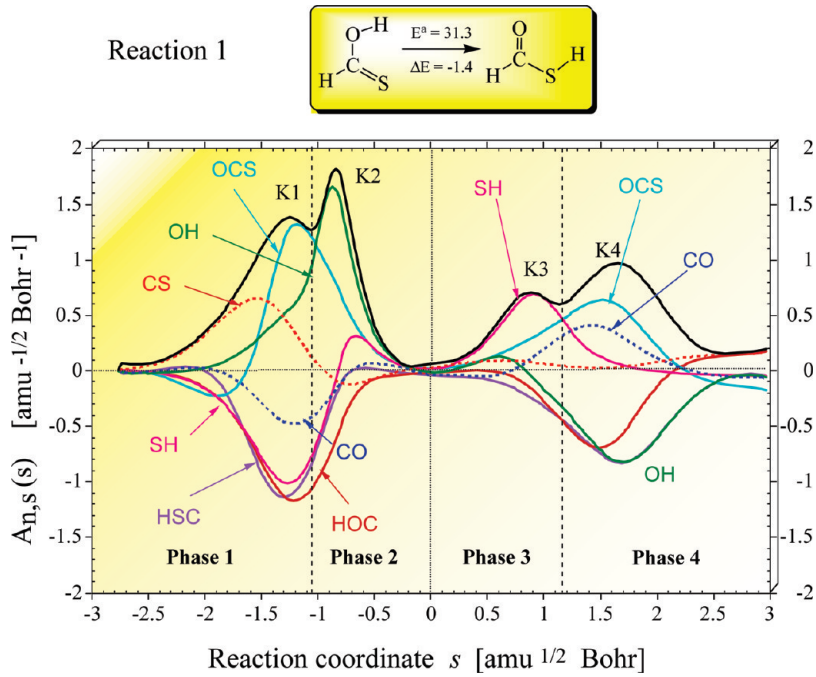


**FIGURE 4.** Curvature diagram for reaction 1: S═C(H)OH → HSC(H)═O. The scalar curvature, $k(s)$, is given as a black line; the adiabatic curvature coupling coefficients, $A_{n,s}(s)$, are given as colored lines. K1−K4 denote the curvature peaks. Vertical lines separate the reaction phases. The transition state is located at $s = 0$ amu $^{1/2}$Bohr. B3LYP/6-311G(d,p) calculations.

ter reveal whether an adiabatic motion of the reaction complex supports ($A_{n,s} > 0$) or resists ($A_{n,s} < 0$) a curving of the reaction path and by this the changes in the reaction complex.[8,11] Analysis of electron density features (difference densities, atom and bond densities, etc.) and other properties of the reaction complex in dependence of $s$ complements a detailed description of the phases of a chemical reaction.[8,11−18]

## 4. The Reaction Phase Diagram and Chemical Predictions

A simple H-transfer reaction between a donor atom and an acceptor atom may illustrate the URVA analysis leading to a dissection of the mechanism into reaction phases. In Figure 4, the curvature diagram of the 1,3 intramolecular H transfer in methanethioic O-acid yielding methanethioic S-acid (thioformic acid): S═C(H)OH → HSC(H)═O (reaction 1) is shown.

According to B3LYP/6-311G(d,p) calculations, reaction 1 proceeds via a barrier of 31.3 kcal/mol and is slightly exothermic (−1.4 kcal/mol). The mechanism was previously investigated by Toro-Labbe and co-workers using the Hellmann−Feynman reaction force, $F(s)$ to dissect the reaction path into a reactant, transition state, and product phase.[21]

The curvature diagram contains four curvature peaks K1−K4 thus leading to a partitioning into four reaction phases. With the help of the adiabatic curvature coupling constants, $A_{n,s}(s)$ (Figure 4), each curvature peak is related to adiabatic vibrational modes: K1 to the OCS and HOC bending modes, K2 to the OH stretching mode, K3 to the SH stretching mode, and K4 again to the OCS bending but also to the HSC bending modes.

One could argue that the H transfer in reaction 1 depends on the donor/acceptor capacities of O and S atoms and therefore any change in the reactant that enhances these capacities will influence mechanism and energetics of reaction 1. The mechanistic picture developing from the curvature diagram $k(s)$ speaks however a different language. The reaction is initiated by deformation of the OCS skeleton (phase 1, light blue line, Figure 4), which first resists and then supports a curving of the reaction path. Bending triggers a lengthening of the C═S bond (red line) and a bending of HOC (brown line). OCS and HOC bending trigger the start of OH bond cleavage (phase 2) and the forming of the SH bond. In phase 3, the SH bond formation is finalized. According to this mechanism, the energy barrier will increase if the ACB (A, B = O, S) heavy atom framework is made more rigid rather than by decreasing the H-acceptor capacity of B. For example replacing S by O leads to a 3 kcal/mol increase (rather than decrease) in the barrier whereas exchanging O against S reduces the barrier. In both cases, the four-phase mechanism shown in Figure 4 is not changed.

The reverse reaction 1 follows the same mechanistic pattern: skeleton deformation (phase 4, Figure 4) as indicated by a large OCS adiabatic curvature coupling constant (complemented now by a HSC bending and CO lengthening contributions) precedes the SH bond cleavage (phase 3). The lower height of K4 (compared with K1) indicates that the OCS bending potential of thioformic acid is less stiff (lower adiabatic bending force constant), the corresponding vibrational modes possesses a larger displacement amplitude, and the thioformic acid minimum is more shallow than that of its isomeric counterpart. Similarly, the heights of K2 and K3 can be related to the strength and stiffness of OH (higher) and SH bonds (lower).

Since the chemical processes of bond cleavage and bond formation take place simultaneously in phases 2 and 3 (a large OH *A*-coefficient is complemented by a small SH *A*-coefficient and vice versa), it is justified to combine these two phases to a transition state phase and to consider phases 1 and 4 as reactant or product preparation phases thus leading to the *E*-based three-phase mechanism of Toro-Labbe and co-workers.[21]

Using URVA, we investigated the hydrogenation of $XH_n$ radicals (F, OH, $NH_2$, $CH_3$),[11] as well as cycloaddition reactions such as the Diels–Alder reaction,[16] the addition of HX or $X_2$ to ethene (X = F, Cl, Br, or I),[15] 1,2 H-shifts in carbenes,[17] and chelotropic reactions such as the addition of methylene (carbenes) to ethene or acetylene.[12,18] In all these reactions, a detailed mechanism based on the reaction phase model could be established. By establishment of this mechanism for a prototypical reaction, for example, the addition of methylene to ethene, predictions of the mechanism and the energetics of related reactions, for example, the addition of carbenes, silylenes, germylenes, etc. to multiple bonds in general, could be made.[18] Also relations between reactions that are generally considered to belong to different reaction types could be established. It was shown that symmetry-forbidden cycloaddition reactions can start as a substitution reaction and terminate as a recombination reaction where the substitution step is responsible for the high energy requirements of the reaction.[15]

The relationship between path curvature, adiabatic force constants, and structural changes of the reaction complex becomes obvious from Figure 5, which shows the curvature diagram of reaction 2, $CH_3 + H_2 \Leftrightarrow CH_4 + H$. The unpaired electron in the $sp^3$-hybrid orbital of the methyl radical extends more into space than the s-electron of the H atom. Accordingly, the far-range polarizing power of the methyl radical is larger than that of H. Despite the fact that the HH bond is

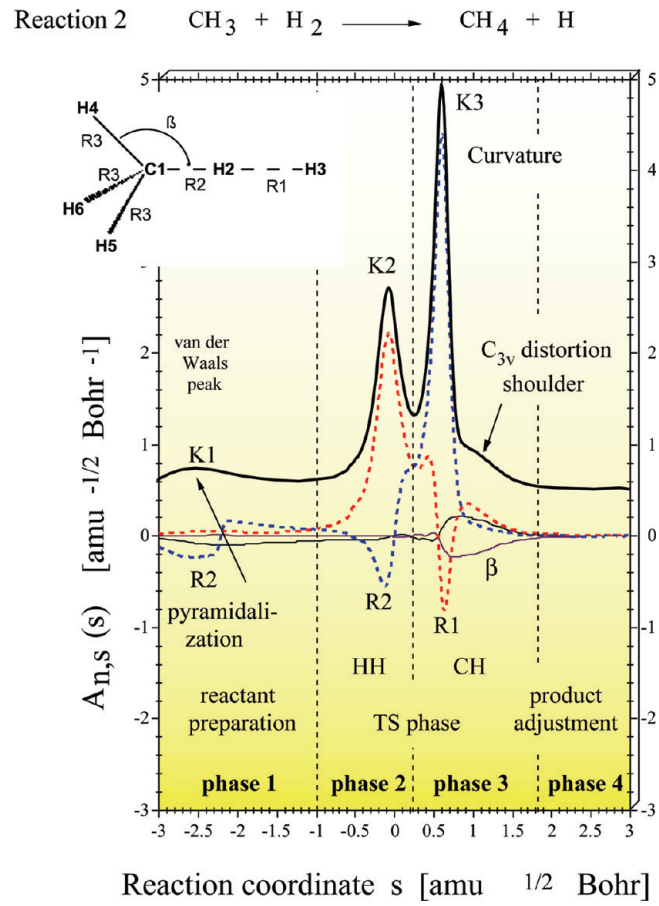


**FIGURE 5.** Decomposition of the reaction path curvature, $k(s)$ (bold black line), of reaction 2 in terms of adiabatic curvature coupling coefficients, $A_{n,s}(s)$ (colored lines). The curvature, $k(s)$, has been shifted by 0.5 units to more positive values to facilitate the distinction between $k(s)$ and $A_{n,s}(s)$. The position of the transition state corresponds to $s = 0$ amu $^{1/2}$Bohr. UMP2/6-31G(d,p) calculations.[11]

stronger than the CH bond in $CH_4$, curvature peak K2 (associated with the HH bond) is broader and smaller than K3 (associated with the CH bond, Figure 5) because under the polarizing power of the methyl radical the HH bond starts earlier to deform and polarizes more smoothly. If a C–H bond in $CH_4$ is attacked by an H atom, deformation of methane begins at close range, which is reflected in the curvature diagram of Figure 5 by a shoulder preceding the CH-cleavage peak K3. K3 is high and rather narrow because the actual cleavage process starts late as reflected by a large adiabatic curvature coupling coefficient, $A_{CH,s}(s)$, and a large derivative $f'_{a,CH}(s)$. If H is replaced by a more polarizing agent such as F, the cleavage peak will become broader and smaller.

The curvature diagram and the mechanism of symmetry-allowed pericyclic reactions differ considerably from those of symmetry-forbidden reactions. This was demonstrated for the Diels–Alder reaction between ethene and butadiene (reac-

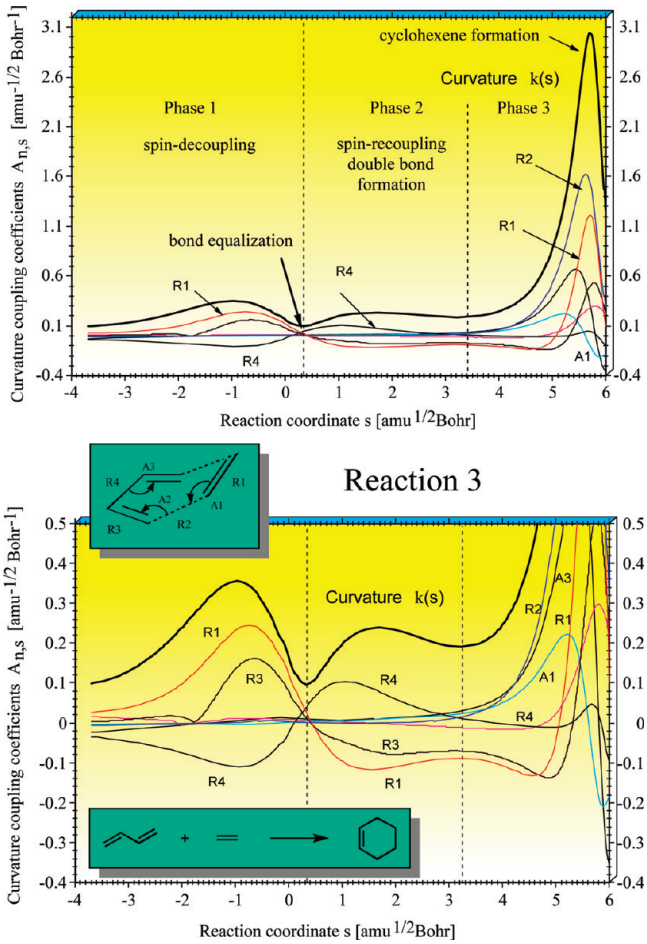


**FIGURE 6.** Curvature diagram (top; bottom shows an enlarged portion) for a symmetry-allowed reaction, the Diels–Alder reaction (reaction 3). B3LYP/6-31G(d,p) calculations.[16]

tion 3), for which the mechanism dissects into three reaction phases (Figure 6):[16] In phase 1, electron spin decoupling of the $\pi$-bonds leads to bond equalization (R(CC) = 1.4 Å) shortly after the transition state at $s = 0$ amu $^{1/2}$Bohr. In phase 2, spin-recoupling results in the formation of a 2-butene structure with some 1,4-biradical character due to pyramidalization of the terminal $CH_2$ groups, which has as a counterpart a similarly distorted ethene molecule (CC bond lengthened and $CH_2$ groups pyramidalized). In phase 3, located far out in the exit channel of the reaction, two new CC bonds and the cyclohexene molecule are formed (Figure 6).

The curvature peaks in phases 1 and 2 close to the transition state are rather small and develop from changes in almost all adiabatic curvature coupling coefficients of the reaction complex. Similar situations are found for other symmetry-allowed pericyclic reactions and suggest a collective but small change of all or most of the internal coordinates of an easy to polarize reaction complex close to the transition state. Such a collective change of many internal coordinates requires less energy than the large change of just a few internal coordinates observed in symmetry-forbidden reactions.[15] Hence, the energy increase toward the transition state is moderate and a relatively low reaction barrier results. Also typical of a symmetry-allowed reaction is the fact that close to the transition state a largely delocalized electron system with equalized heavy atom bonds is generated. This is in line with the Dewar–Evans–Zimmermann rules that compare the transition state of a symmetry-allowed pericyclic reaction with aromatic cyclopolyenes benefiting from electron delocalization.

## 5. Hidden Intermediates and Hidden Transition States

The mechanism of the symmetry-forbidden cycloaddition reaction between ethene and HF (reaction 4, $CH_2{=}CH_2 + FH \rightarrow CH_3CH_2F$) is characterized by four curvature peaks and four reaction phases (van der Waals peak K1 and van der Waals phase are not shown) that indicate HF cleavage, CH bond formation (phases 2 + 3), and CF bond formation (phase 4).[15] The transient configuration of the reaction complex at $s = 2.7$ amu $^{1/2}$Bohr resembles an ethyl cation separated from a F anion according to geometry and charge distribution.[15] If this transient structure is stabilized in a polar nonprotic solvent or F is exchanged against Br or I in the reaction complex, a real intermediate is obtained, which justifies to speak in the case of the gas-phase reaction 4 of the presence of a *hidden intermediate*.[15,18]

Figure 7 shows (a) energy profile, $E(s)$, (b) curvature diagram, $k(s)$, and three reaction phases of the chelotropic cycloaddition of $CH_2(^1A_1)$ to ethene yielding cyclopropane (reaction 5).[18] The reaction proceeds without any barrier in a single, strongly exothermic step where $E(s)$ does not offer much mechanistic insight. However, analysis of the reaction path curvature reveals a complicated mechanism comprising four different mechanistic phases (including the van der Waals phase not shown in Figure 7). Between the phases, a *hidden transition state* (corresponding to a single CC bond formation) and a *hidden intermediate* (corresponding to a trimethylene biradical) are located that can convert to a real transition state or intermediate in the case of other carbenes, silylenes, or germylenes, as was demonstrated for the reaction between difluorocarbene and ethene or the reaction between germylene and ethene.[18] The URVA analysis of the mechanism of the prototypical reaction 5 makes it possible to predict the mechanism of other chelotropic cycloaddition reactions in differ-

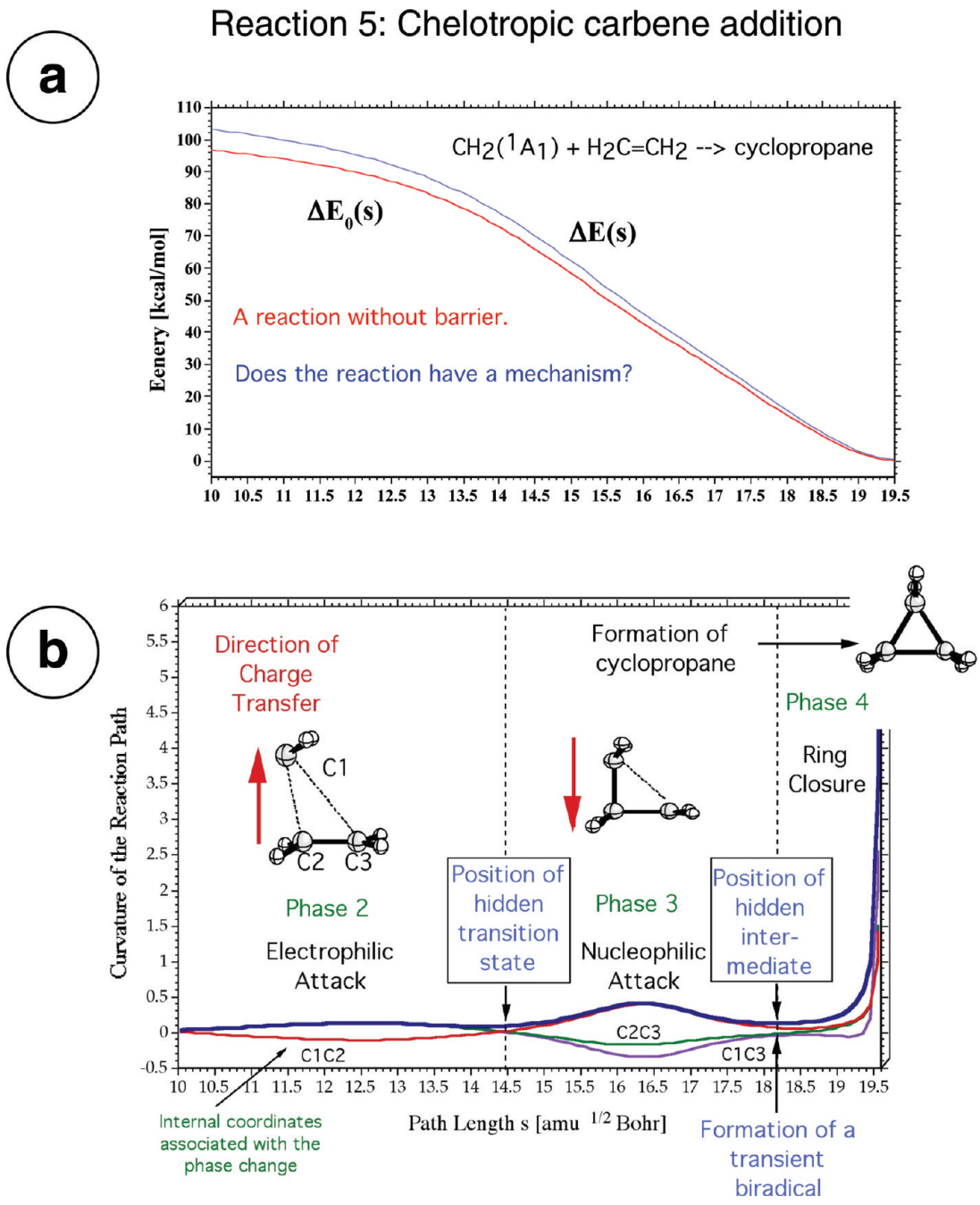


**FIGURE 7.** Energy profiles $E(s)$ and $E_0(s) = E(s) + \text{ZPE}$ (top) and curvature diagram (bottom) of the barrierless reaction 5: $CH_2(^1A_1) + H_2C{=}CH_2 \rightarrow$ cyclopropane. Curvature (blue), some of the adiabatic curvature coupling coefficients (green, red, purple), and reaction phases (except van der Waals) are shown. B3LYP/6-31G(d,p) calculations.[18]

ent environments thus opening up a new way of understanding and controlling chemical reactions.

## 6. Conclusions

Previous work on chemical reaction mechanism focused almost exclusively on the stationary points of the PES along the reaction path, thus overemphasizing the role of the total energy $E(s)$, which as a collective quantity cannot provide detailed insight into the mechanism. The details of the mechanism are unraveled when analyzing changes in the structure of the reaction complex. Due to the relationship between reaction complex and reaction path, analysis of reaction path direction and curvature in terms of adiabatic vibrational modes leads to the dissection of the mechanism into reaction phases where the chemically important changes of the reaction complex take place. Even a one-step reaction with-

out a transition state (dissociation of $H_2$; addition of methylene to ethene) possesses a nontrivial mechanism and encounters two or more reaction phases along the reaction path. The analysis of the mechanism in terms of reaction phases for prototypical chemical reactions reveals that the chemical processes of bond breaking and forming can take place close to the transition state or far away in exit and entrance channel. The fate of a reaction is determined in the van der Waals phase.[15] The adiabatic curvature coupling coefficients describing chemical processes can be related to bond strength as probed under the polarizing ability of an attacking reaction partner. Specific transient points along the reaction path associated with a curvature minimum can be converted to stationary points (transition state or minimum) if the reaction complex or the reaction conditions are changed in a specific way. Therefore, it is justified to call these transient points *hidden intermediates* or *hidden transition states*. Examples have been given for the cycloaddition of HX to multiple bonds and the chelotropic addition of carbenes to ethene.[15,18]

The analysis of the mechanism of a chemical reaction as described in this Account bears a large potential. Current work in this research area aims at the quick comparison of dozens of chemical reactions, including the reactions of biomolecules, reactions in solution, and homogenously or heterogeneously catalyzed reactions (reactions on surfaces), which is supported by the development of more efficient reaction path following methods.[33] These investigations will lead to new insights and advance chemistry toward a control of chemical reactions as needed for the energy-conserving production of new materials under environment-protecting conditions.

*The authors thank Prof. W. Quapp, Prof. A. Toro-Labbe, Dr. R. Pandei, Dr. H. Joo, and Dr. D. Izotov for useful discussions. Financial support by the National Science Foundation, Grant CHE 071893, is acknowledged.*

## BIOGRAPHICAL INFORMATION

**Prof. Dr. Elfi Kraka** worked five years at Bayer Leverkusen, Germany, before studying chemistry at the University of Köln, Germany. She carried out postdoctoral studies on reaction mechanism and dynamics at Argonne National Laboratory under the supervision of Prof. Thom Dunning. She became assistant professor and later full professor in Theoretical Chemistry at the University of Göteborg. Since 2009, she has been working at Southern Methodist University, Dallas, Texas, as professor and chair of chemistry. Her research in the area of computer-assisted drug design, molecular modeling, reaction dynamics, and reaction mechanism is summarized in more than 130 peer-refereed publications.

**Prof. Dr. Dieter Cremer** studied Chemistry at the University of Cologne, Germany. After his Ph.D., he worked with Nobel Laureate John Pople on the development and application of ab initio methods at Carnegie-Mellon University. In 1979, he finished his habilitation work on the *Ab initio investigation of reaction mechanism* and became first Privat-Dozent and later Heisenberg-Professor for Theoretical Chemistry at the University of Cologne. From 1990 on, he was the scientific director of the newly founded Theoretical Chemistry Section of the University of Göteborg, Sweden. Since 2009, he has been professor of Computational and Theoretical Chemistry at Southern Methodist University, Dallas, Texas. His research interests include the development of quantum chemical methods, their application to molecular problems, and the study of reaction mechanism, materials sciences, and nanotechnology as is documented in more than 300 peer-refereed publications.

## REFERENCES

1 Lowry, T. H.; Schueller Richardson, K. *Mechanism and Theory in Organic Chemistry*; Harper&Row: New York, 1987.

2 *Organic Reaction Mechanisms, 1965−2004*; Knipe, A. C, Watts, W. E., Eds.; Wiley: New York, 2008.

3 *Encyclopedia of Computational Chemistry*; Schleyer, P.v.R., Allinger, N. L., Clark, T., Gasteiger, J., Kollman, P., Schaefer, H. F., III, Schreiner, P. R., Eds.; John Wiley: Chichester, U.K., 1998.

4 Steinfeld, J. L.; Francisco, J. S.; Hase, W. L. *Chemical Kinetics and Dynamics*; Prentice Hill: London, 1999.

5 Fukui, K. The path of chemical-reactions - the IRC approach. *Acc. Chem. Res.* **1981**, *14*, 363–368.

6 Cremer, D.; Crehuet, R.; Anglada, J. The ozonolysis of acetylene - a quantum chemical investigation. *J. Am. Chem. Soc.* **2001**, *123*, 6127–6141.

7 Miller, W. H.; Handy, N. C.; Adams, J. E. Reaction path Hamiltonian for polyatomic molecules. *J. Chem. Phys.* **1980**, *72*, 99–112.

8 Kraka E., Reaction path Hamiltonian and its use for investigating reaction mechanism. In *Encyclopedia of Computational Chemistry*. Schleyer, P.v.R. Allinger, N. L., Clark, T., Gasteiger, J., Kollman, P. A., Schaefer, H. F., III, Schreiner, P. R., Eds.; John Wiley: Chichester, U.K., 1998; Vol. 4, pp 2437−2463.

9 Kraka, E.; Dunning, T. H., Jr. Characterization of molecular potential energy surfaces: critical points, reaction paths and reaction valleys. In *Advances in Molecular Electronic Structure Theory: The Calculation and Characterization of Molecular Potential Energy Surfaces*; Dunning. T. H., Jr., Ed; JAI Press, Inc.: Greenwich, CT, 1990; pp 129−173.

10 Konkoli, Z.; Cremer, D.; Kraka, E. Diabatic ordering of vibrational normal modes in reaction valley studies. *J. Comput. Chem.* **1997**, *18*, 1282–1289.

11 Konkoli, Z.; Kraka, E.; Cremer, D. Unified reaction valley approach: Mechanism of the reaction $CH_3 + H_2 \Leftrightarrow CH_4 + H$. *J. Phys. Chem. A* **1997**, *101*, 1742–1757.

12 Quapp, W.; Kraka, E.; Cremer, D. Finding the transition state of quasi-barrierless reactions by a growing string method for Newton trajectories: Application to the dissociation of methylenecyclopropene and cyclopropane. *J. Phys. Chem. A* **2007**, *111*, 11287–11293.

13 Dunning, T. H., Jr; Kraka, E; Eades., R. A. Insights into the mechanism of chemical reactions. Reaction paths for chemical reactions. *Faraday Discuss. Chem. Soc.* **1987**, *84*, 427–440.

14 Dunning, T. H., Jr.; Harding, L. B.; Kraka, E. Calculation and characterization of reaction valleys for chemical reactions. In *NATO Advanced Research Workshop on Supercomputer Algorithms for Reactivity, Dynamics and Kinetics of Small Molecules*; Kluwer Academic Publishers: Dordrecht, the Netherlands, 1989; pp 57−68.

15 Cremer, D.; Wu, A.; Kraka, E. The mechanism of the reaction $FH + H_2C{=}CH_2 \rightarrow H_3C{-}CFH_2$: Investigation of hidden intermediates with the unified reaction valley approach. *Phys. Chem. Chem. Phys.* **2000**, *3*, 674–687.

16 Kraka, E.; Wu, A.; Cremer, D. The mechanism of the Diels−Alder reaction studied with the united reaction valley approach: Mechanistic differences between symmetry-allowed and symmetry-forbidden reactions. *J. Phys. Chem. A.* **2003**, *107*, 9008–9021.

17 Kraka, E.; Cremer, D. Mechanism and dynamics of organic reactions: 1,2-H shift in methylchlorocarbene. *J. Phys. Org. Chem.* **2002**, *15*, 431–447.

18 Joo, H.; Kraka, E.; Quapp, W.; Cremer, D. The mechanism of a barrierless reaction: Hidden transition state and hidden intermediates in the reaction of methylene with ethene. *Mol. Phys.* **2007**, *105*, 2697–2717.

19 Quapp, W.; Heidrich, D. Analysis of the concept of minimum energy path on the potential energy surface of chemically reacting systems. *Theor. Chim. Acta* **1984**, *66*, 245–260.

20 See, for example: Quapp, W. Chemical reaction paths and calculus of variations. *Theor. Chem. Acc.* **2008**, *121*, 227–237, and references therein.

21 Gutierrez-Oliva, S.; Herrera, B.; Toro-Labbe, A; Chermette, H. On the mechanism of hydrogen transfer in the HSCH(═O) ⇌ (S)CHOH and HSNO ⇌ SNOH reactions. *J. Phys. Chem. A* **2005**, *109*, 1748–1751.

22 Toro-Labbe, A; Gutierrez-Oliva, S.; Murray, J. S.; Politzer, P. A new perspective on chemical and physical processes: The reaction force. *Mol. Phys.* **2007**, *105*, 2619–2625.

23 Kato, S.; Morokuma, K. Potential energy characteristics and energy partitioning in chemical reactions: Ab initio MO study of $H_2CCH_2F \rightarrow H_2CCHF + H$ reaction. *J. Chem. Phys.* **1980**, *73*, 3900–3915.

24 Page, M.; McIver, J. W., Jr. On evaluating the reaction path Hamiltonian. *J. Chem. Phys.* **1988**, *88*, 922–935.

25 Konkoli, Z.; Cremer, D. A new way of analyzing vibrational spectra I. Derivation of adiabatic, internal modes. *Int. J. Quantum Chem.* **1998**, *67*, 1–9.

26 Konkoli, Z.; Cremer, D. A new way of analyzing vibrational spectra II. Comparison of internal mode frequencies. *Int. J. Quantum Chem.* **1998**, *67*, 11–27.

27 Konkoli, Z.; Cremer, D. A new way of analyzing vibrational spectra III. Characterization of normal vibrational modes in terms of internal vibrational modes. *Int. J. Quantum Chem.* **1998**, *67*, 29–40.

28 Konkoli, Z.; Larsson, A.; Cremer, D. A new way of analyzing vibrational spectra IV. Application and testing of adiabatic modes within the concept of the characterization of normal modes. *Int. J. Quantum Chem.* **1998**, *41*−*65*, 1–9.

29 Cremer, D.; Larsson, A. J.; Kraka, E. New developments in the analysis of vibrational spectra: On the use of adiabatic internal vibrational modes. In *Theoretical Organic Chemistry*; Parkanyi, C., Ed.; Theoretical and Computational Chemistry, Volume *5*; Elsevier: Amsterdam, 1998; pp259−327.

30 Larsson, J. A.; Cremer, D. Theoretical verification and extension of the McKean relationship between bond lengths and stretching frequencies. *J. Mol. Struct.* **1999**, *485*, 385–407.

31 Kraka, E.; Cremer, D. Characterization of CF bonds with multiple-bond character: Bond lengths, stretching force constants, and bond dissociation energies. *Chem. Phys. Chem.* **2009**, *10*, 686–698.

32 Cremer, D; Kraka, E. From molecular vibrations to bonding, chemical reactions, and reaction mechanism. *Curr. Org. Chem.*, **2010**, in press.

33 See, for example: Hratchian, H. P.; Schlegel, H. B. Using Hessian updating to increase the efficiency of a Hessian based predictor-corrector reaction path following method. *J. Chem. Theory Comput.* **2005**, *1*, 61–69.